Electronic Supplementary Material (ESI) for Materials Chemistry Frontiers.

Exploring the potential of linear polymer structures for the synthesis of fluorescent gold nanoclusters

*Nik Nik Mohd Adnan[a], Syafiq Ahmad[a], Rhiannon P. Kuchel[c], Cyrille Boyer[a]**

[a]Australian Centre for Nanomedicine (ACN), School of Chemical Engineering, University of New South Wales, Sydney, Australia 2052. E-mail: cboyer@unsw.edu.au

[b]Centre for Advanced Macromolecular Design (CAMD), School of Chemical Engineering, University of New South Wales, Sydney, Australia 2052. E-mail: cboyer@unsw.edu.au

[c]Electron Microscope Unit (EMU), Mark Wainwright Analytical Centre, University of New South Wales, Sydney, Australia 2052.

Supplementary figures

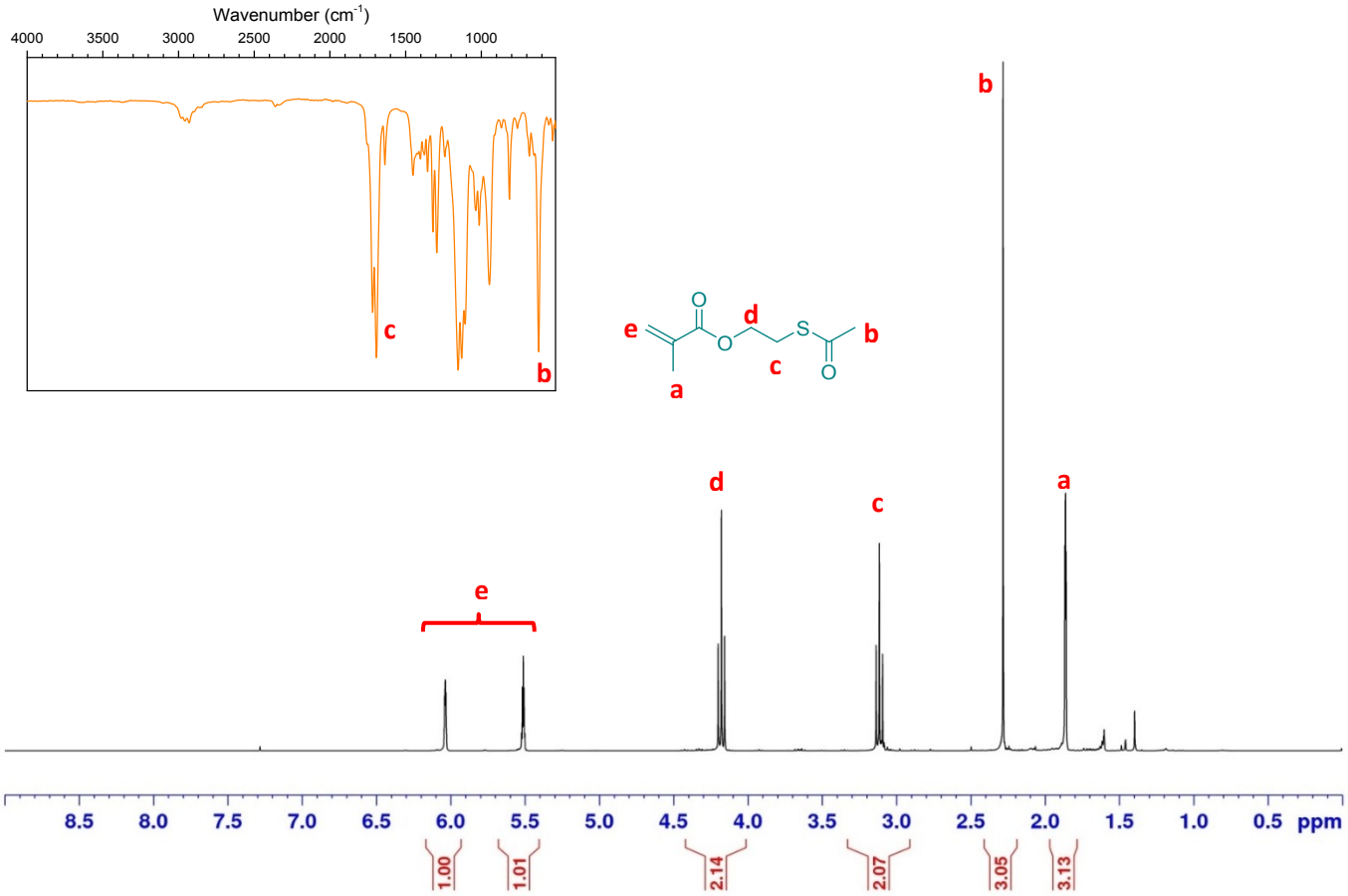

Figure S1. ^{1}H-NMR of purified 2-(acetylthio)ethyl methacrylate (AcSEMA) in $CDCl_3$. Inset: ATR-FTIR spectrum of AcSEMA showing the presence of signal b, methyl thioester and c, thioester.

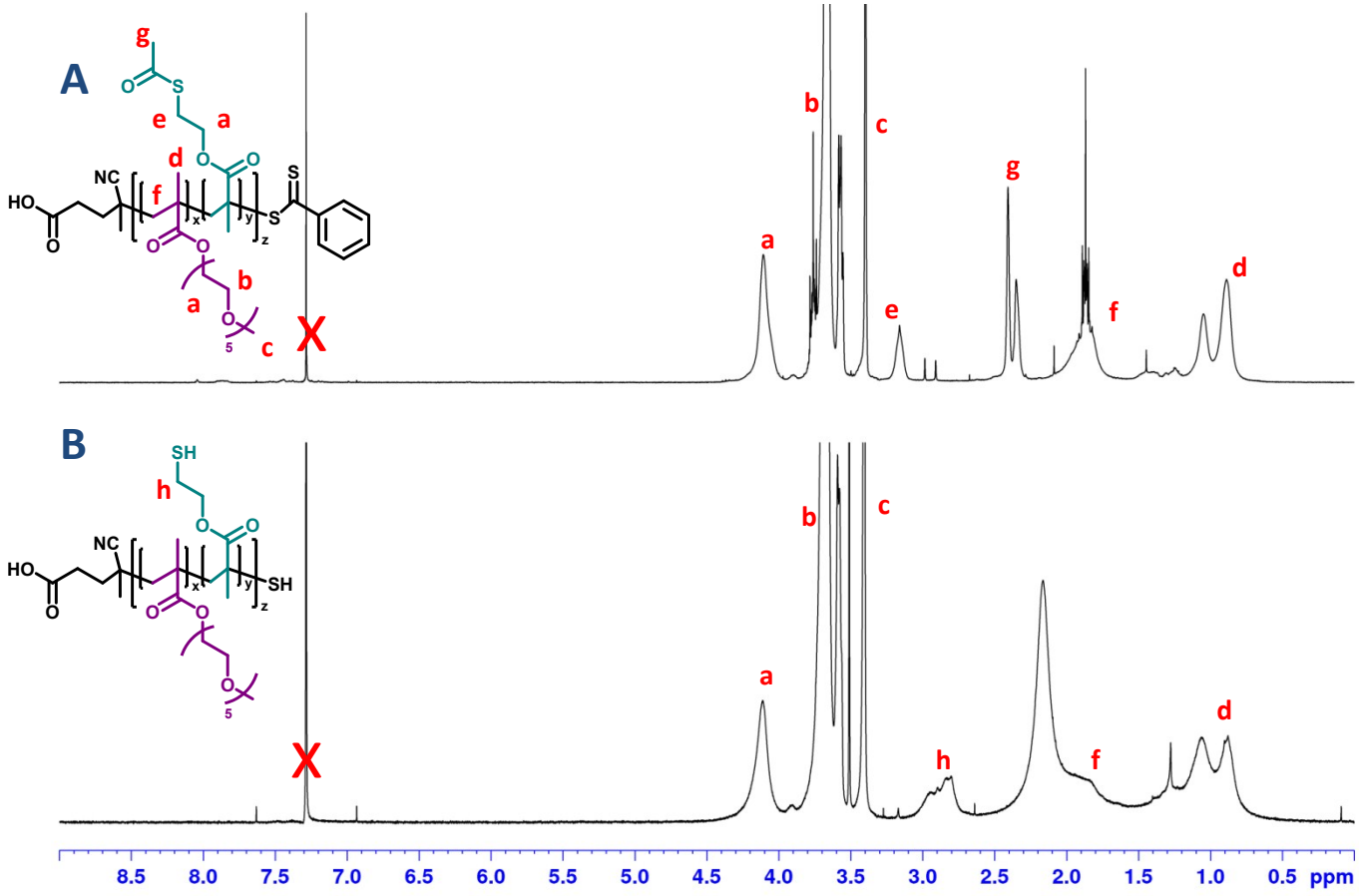

Figure S2. ^{1}H-NMR analysis of (A) P(OEGMA-*co*-AcSEMA) in $CDCl_3$ and (B) P(OEGMA-*co*-MEM) in $CDCl_3$

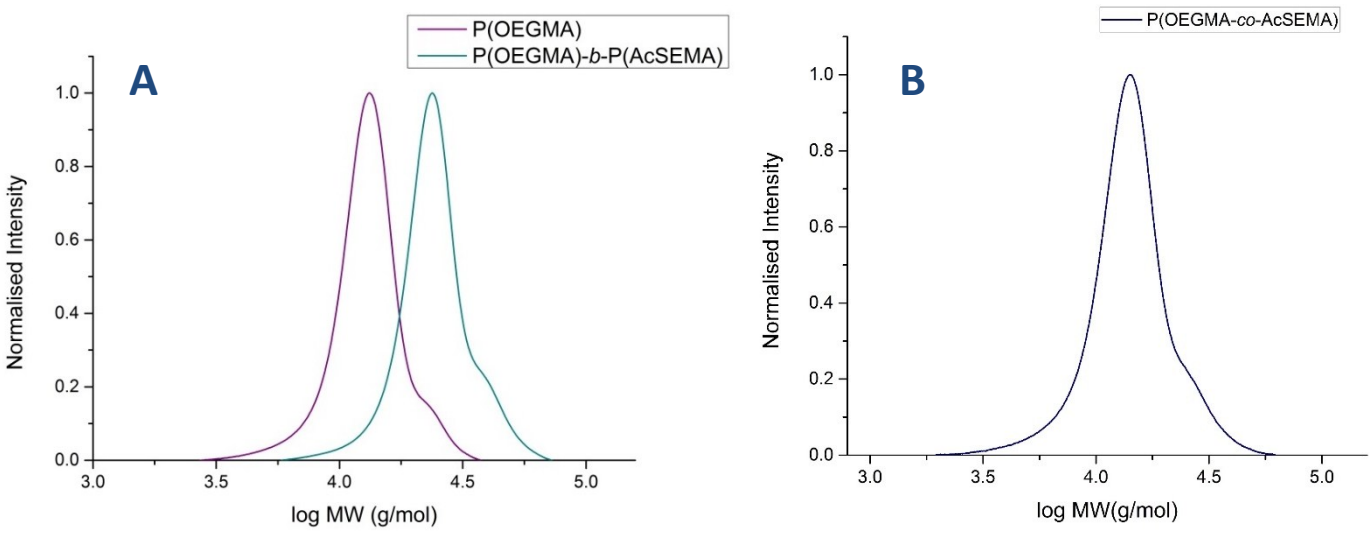

Figure S3. SEC spectra of the (A) homopolymer P(OEGMA) and block copolymer P(OEGMA)-*b*-P(AcSEMA) (B) random copolymer P(OEGMA-*co*-AcSEMA)

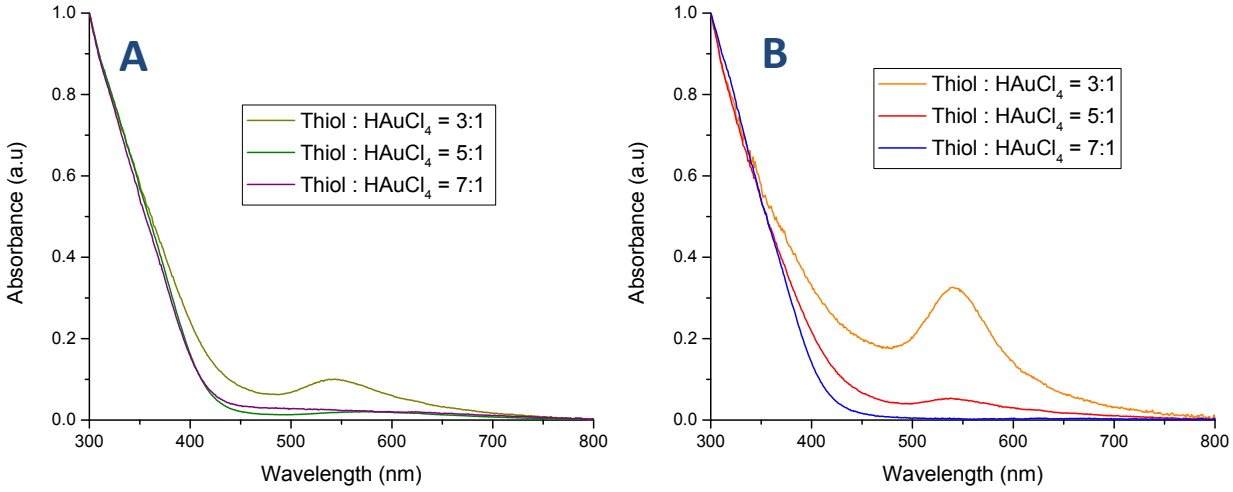

Figure S4. UV-vis spectra of the (A) B@AuNCs (B) R@AuNCs before purification. The formation of a side product such as non-fluorescent gold nanoparticles can be observed by the appearance of the characteristic absorbance of the localised surface plasmon resonance. The amount of side product decreases as the relative molar concentration of polymer to gold increases.

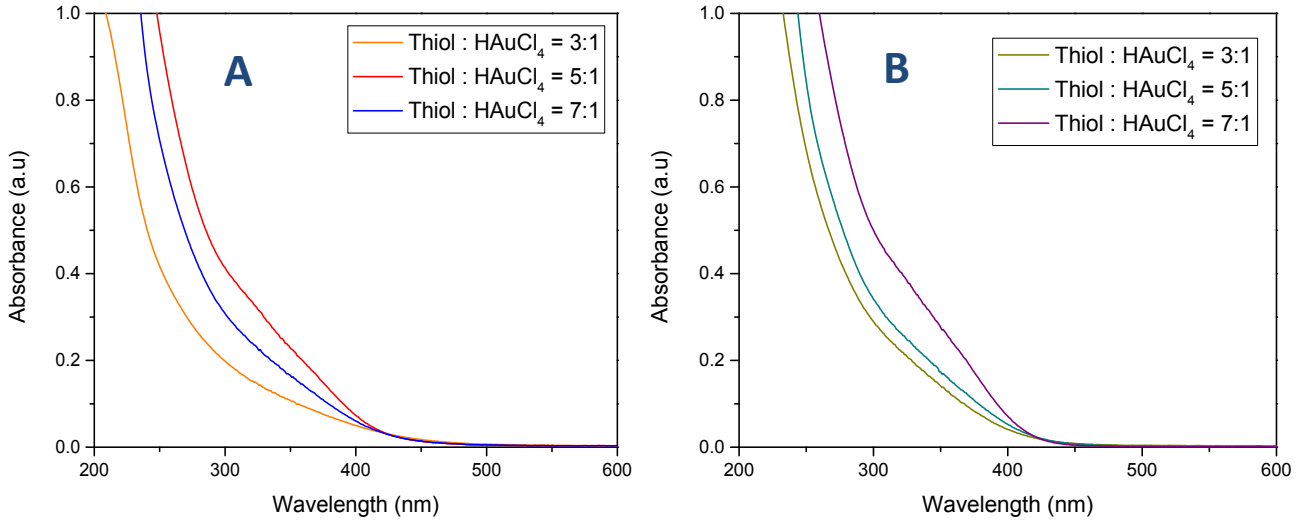

Figure S5. UV-vis spectra of the (A) B@AuNCs (B) R@AuNCs showing the purified gold nanoclusters and successful removal of bigger gold nanoparticles and aggregates by the absence of the localised surface plasmon resonance characteristic absorbance.

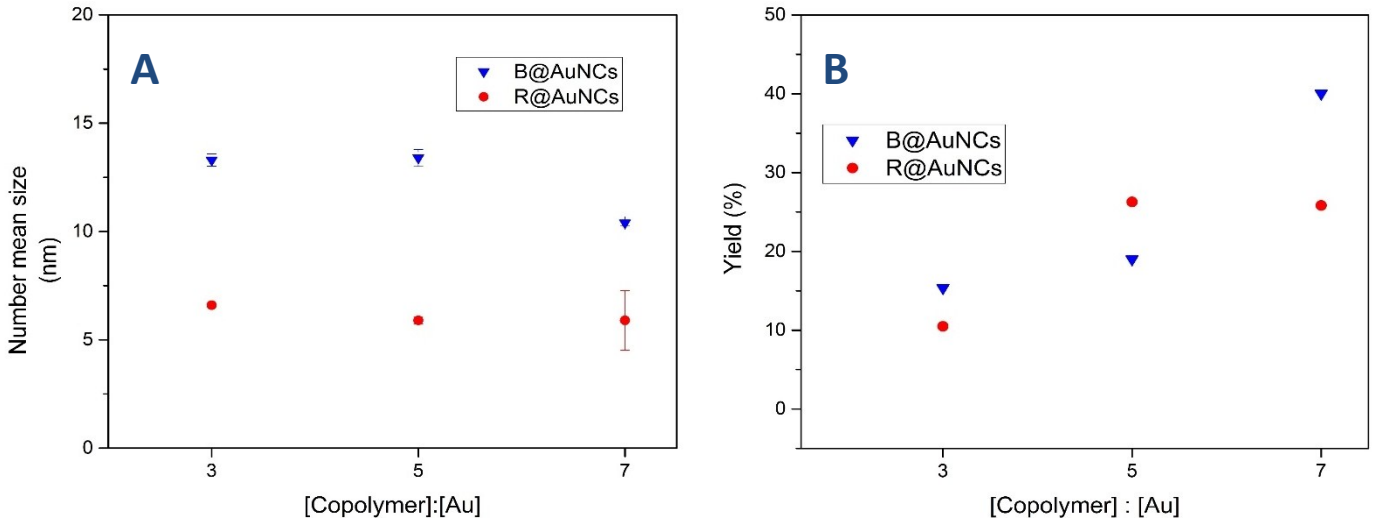

Figure S6. (A) Number-mean size of the AuNCs at different relative molar concentration of polymer to gold determined by dynamic light scattering (DLS) (B) Yield of the AuNCs calculated from the relative gold concentration obtained by ICP-OES and starting gold concentration.

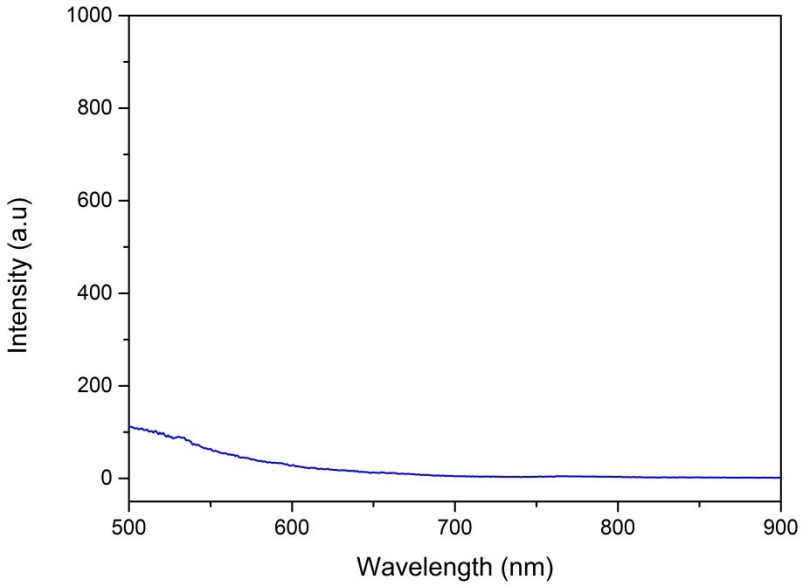

Figure S7. Fluorescence emission spectra of the copolymer in water.

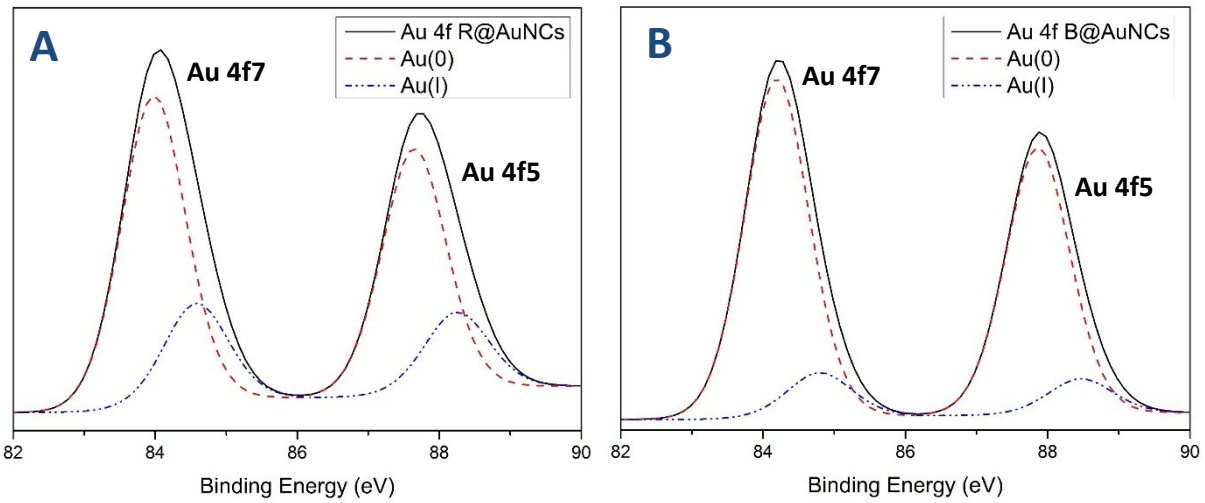

Figure S8. Au 4f spectra as determined by XPS and the deconvolution to identify signals attributed to Au(0) and Au(I) of the (A) R@AuNCs (B) B@AuNCs

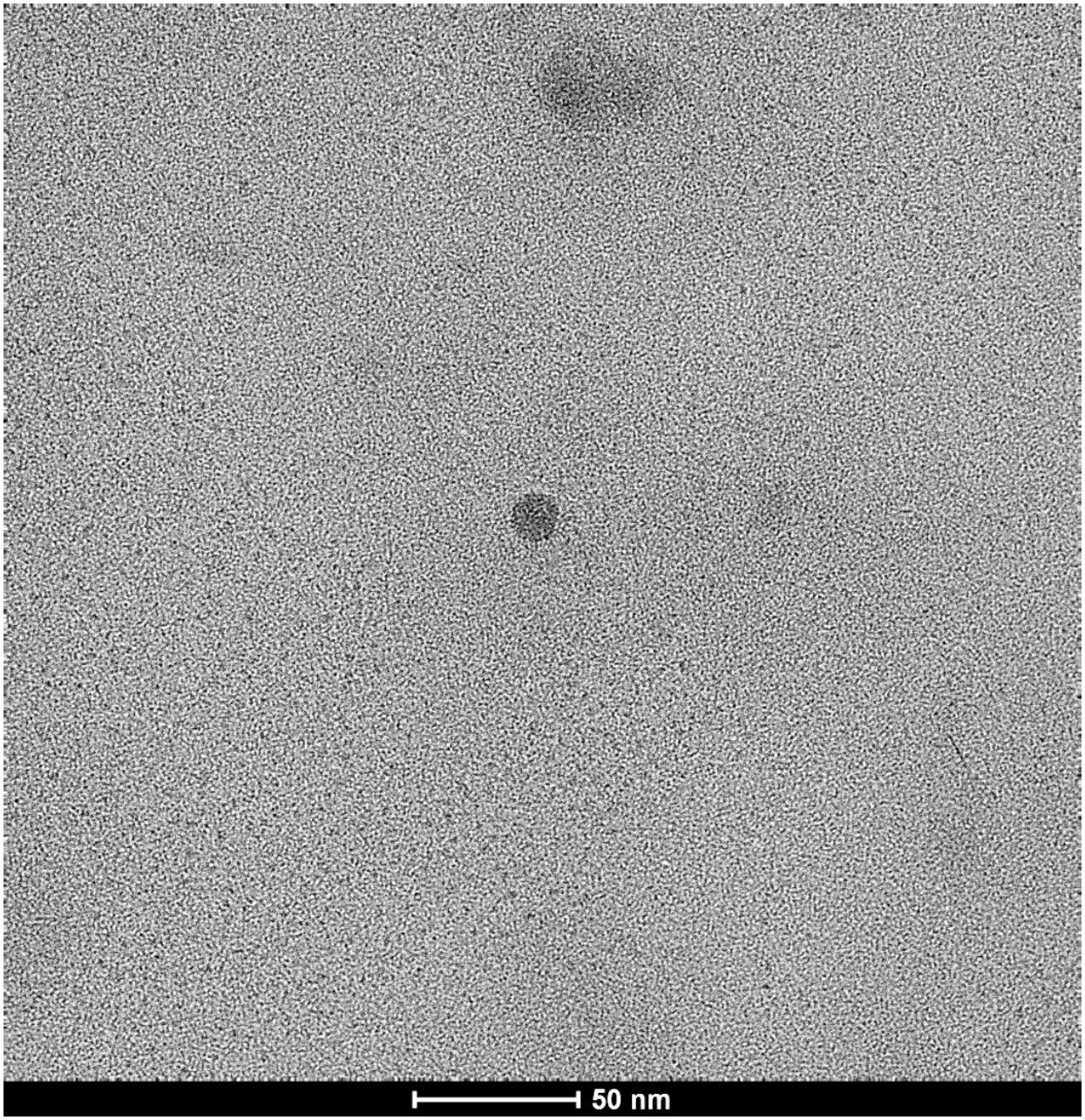

Figure S9. TEM micrograph of the AuNCs (B@AuNCs). Low contrast small dots can be attributed to the AuNCs core which is smaller than 2 nm.

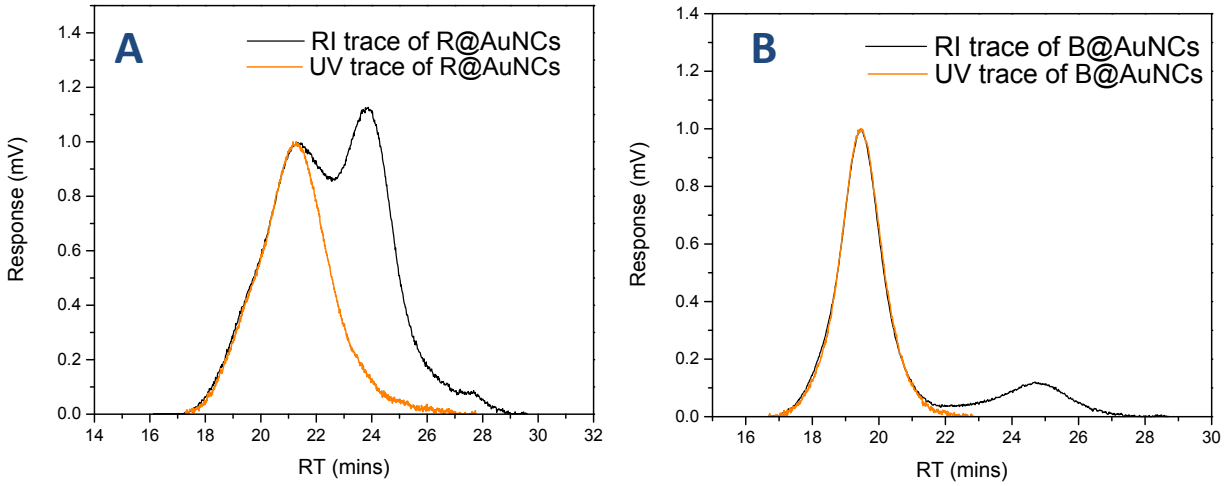

Figure S10. SEC traces of (A) R@AuNCs and (B) B@AuNCs detected by refractive index (RI) and UV (400 nm) detectors showing the formation of higher molecular weight, fluorescent nanostructures compared to their respective single linear copolymers.

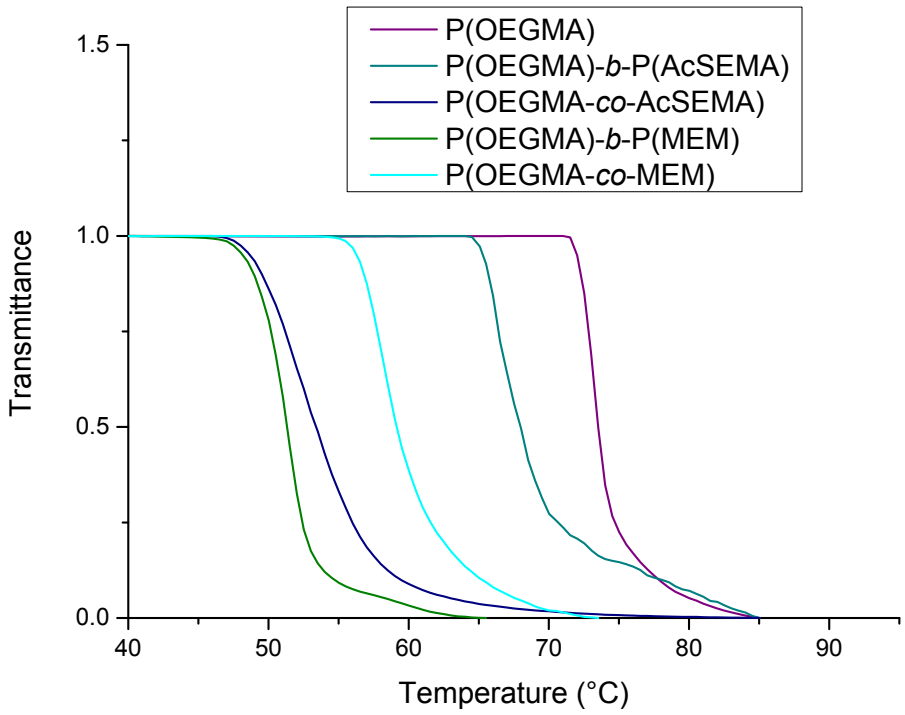

Figure S11. Turbidimetry measurement of the copolymers to determine the lower critical solution temperature (LCST) point by UV-vis spectroscopy.

$$h\nu \cong \frac{E_f}{\sqrt[3]{N}} = \frac{E_f r_s}{R}$$

Equation S1. Jellium Model describes the relation between fluorescence emission of metal nanoclusters and the core size.

h	Planck constant
ν	Emission frequency
E_f	Fermi energy
N	Number of atoms
r_s	Weigner-Seitz radius
R	Radius of nanoclusters core